Quantum Optics of Spin Waves through ac Stark Modulation

Michał Parniak,[1,2,*] Mateusz Mazelanik,[1,2,†] Adam Leszczyński,[1,2] Michał Lipka,[1,2] Michał Dąbrowski,[1,2] and Wojciech Wasilewski[1,2]

[1] *Faculty of Physics, University of Warsaw, Pasteura 5, 02-093 Warsaw, Poland*
[2] *Centre for Quantum Optical Technologies, Centre of New Technologies, University of Warsaw, Banacha 2c, 02-097 Warsaw, Poland*

(Received 10 July 2018; published 14 February 2019)

We bring the set of linear quantum operations, important for many fundamental studies in photonic systems, to the material domain of collective excitations known as spin waves. Using the ac Stark effect we realize quantum operations on single excitations and demonstrate a spin-wave analog of the Hong-Ou-Mandel effect, realized via a beam splitter implemented in the spin-wave domain. Our scheme equips atomic-ensemble-based quantum repeaters with quantum information processing capability and can be readily brought to other physical systems, such as doped crystals or room-temperature atomic ensembles.

DOI: 10.1103/PhysRevLett.122.063604

The Hong-Ou-Mandel (HOM) interference [1] is an inherently quantum two-particle effect serving as an important test of both nonclassicality of the input state as well as proper operation of the beam splitter. While nowadays it is easily achievable with photons, recent experiments demonstrated similar quantum-interferometric properties of atoms [2–4], phonons [5,6], plasmons [7,8], and photons but in elaborate hybrid systems [6,9–14]. This progress illuminates the perspective to combine linear operations, which have always been simple for photons, and nonlinear operations, which can be engineered in material systems. A quantum memory (QM) for light, where photons are stored in the form of collective atomic excitations, is a good candidate for a bedrock to realize this proposal facilitating both fundamental studies and applications in quantum networks. Substantial challenges emerge, however, since photonic quantum networks need to extensively utilize multiplexing techniques, exploring photonic spatial and temporal structure, to achieve high performance [15–19]. Multimode QMs [20–22] can become part of such networks, but a requirement of implementing complex linear operations on stored excitations arises.

In this Letter we harness these material quasiparticles—collective atomic excitations known as spin waves (SWs). We demonstrate that the spatial structure of SWs can be manipulated via the off-resonant ac Stark (ACS) shift. Through SW diffraction-based (cf. Kapitza-Dirac effect [23]) beam splitter transformation, we realize the Hanbury Brown–Twiss (HBT) type measurement in the SW domain [24], demonstrating precise control and nonclassical statistics of atomic excitations. Finally, we observe interference of two SWs—an analog of the HOM effect for photons. Thanks to the reversible photon-SW mapping via the Duan-Lukin-Cirac-Zoller (DLCZ) protocol [25], these techniques enable encoding states from a high-dimensional Hilbert space into the spatial structure of SWs to facilitate not only new quantum communication schemes [26], but also high data rate classical telecommunication [27,28]. A quantum repeater equipped with such coprocessing capability could perform error correction [29–32] or small-scale computation on transmitted quantum data.

The ability to perform beam splitter transformations with wave vector eigenmodes constitutes a full SW analog of complex linear-optical networks. The inherently nonclassical HOM interference with 80% visibility is a concise demonstration of such transformation, which we realize with a three-way (in the sense of the first three diffraction orders) splitter to demonstrate that SWs always occupy either of the output modes. On the fundamental level, the interference of two SWs with different wave vectors demonstrates preservation of coherence of many material quasiparticles in a thermal ensemble. Remarkably, the presented idea along with its applications can be brought to a multitude of physical systems where ACS shift control is feasible, including solids doped with rare-earth ions [33,34], color centers in diamond [35], trapped ions [36], or warm atomic ensembles [37].

We use an elongated ($10 \times 0.3 \times 0.3$ mm^3) cold ^{87}Rb ensemble prepared in a magneto-optical trap (MOT) to generate, store, and process ground-state SWs. Generation of single SWs relies on Raman scattering, which forms the basis of the DLCZ protocol [25]. A scattering event, registered as a "write-out" (w) photon with a wave vector $\mathbf{k}^w$, heralds creation of a single SW excitation with a wave vector $\mathbf{K} = \mathbf{k}^W - \mathbf{k}^w$, where $\mathbf{k}^W$ is the write laser wave vector. The creation operator for a SW with wave vector $\mathbf{K}$ is $\hat{S}^\dagger_{\mathbf{K}} = N^{-1/2} \sum_n^N e^{i\mathbf{K}\cdot\mathbf{r}_n} |h_n\rangle\langle g_n|$, where $|0\rangle = |g_1 \ldots g_N\rangle$ with $N \approx 10^8$ atoms in the ground state [Fig. 1(c)]. One atomic ensemble can accommodate many independent

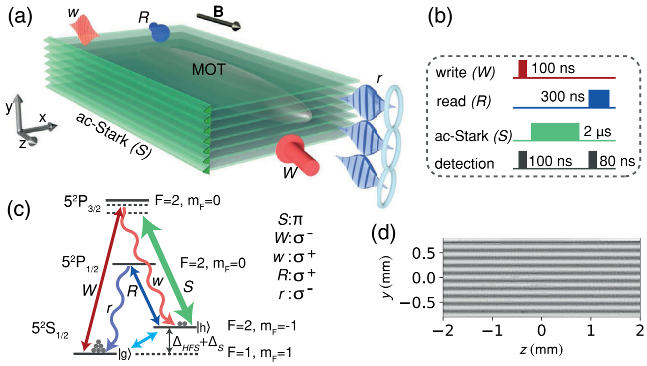

FIG. 1. Experimental setup for generating and manipulating SWs. (a) Detection of a single write-out photon w scattered from write laser W heralds creation of a SW inside the atomic ensemble. The SW is then manipulated using an ACS light pattern (d) generated with a far-detuned laser S. The SW can then be converted by the read laser R to a readout photon r with a reshaped spatial mode. (c) The relevant energy level configuration: $|g\rangle = |5^2S_{1/2}F = 1, m_F = 1\rangle$ and $|h\rangle = |5^2S_{1/2}F = 2, m_F = -1\rangle$. The write laser is red detuned from the $5^2S_{1/2}F = 1 \rightarrow 5^2P_{3/2}F = 2$ transition by 25 MHz, the read laser is resonant with the $5^2S_{1/2}F = 2 \rightarrow 5^2P_{1/2}F = 2$ transition, and the ACS laser S is red detuned from the $5^2S_{1/2}F = 2 \rightarrow 5^2P_{3/2}$ line centroid by 1.43 GHz. During QM operation we keep constant bias magnetic field $\mathbf{B} = (50\ \mathrm{mG})\hat{e}_z$. (b) The sequence revealing the timing of each step during the experiment.

spatial SW modes. For SW detection, we use a read laser R (wave vector $\mathbf{k}^R$) pulse that converts the SW into a "readout" (r) photon with wave vector $\mathbf{k}^r = \mathbf{K} + \mathbf{k}^R$.

To engineer ground-state SWs in our spatially multimode QM we employ an off-resonant strong laser shaped with a spatial light modulator [38] (Fig. 1), inducing a spatially dependent differential ACS shift $\Delta_S(\mathbf{r})$ between levels $|g\rangle$ and $|h\rangle$, directly proportional to light intensity. With negligible absorption and a small transverse size of the ensemble, we assume a constant intensity along the propagation axis x of the S beam and thus write $\Delta_S(\mathbf{r}) = \Delta_S(y, z)$. The ACS shift leads the SWs to accumulate an additional, spatially dependent phase $\varphi_S(y, z) = \Delta_S(y, z)T$ over the interaction time $T \sim 2\ \mu$s with a typical $\Delta_S/2\pi \sim 36$ kHz obtained with 35 mW/cm^2 intensity of S light detuned from the respective resonance by $\delta_S/2\pi = 1.43$ GHz. Such a manipulation is equivalent to the following transformation of the SW creation operator within the Heisenberg picture: $\hat{\hat{S}}^\dagger_{\mathbf{K}} = N^{-1/2}\sum_n^N e^{i\mathbf{K}\cdot\mathbf{r}_n + i\varphi_S(\mathbf{r}_n)}|h_n\rangle\langle g_n| = \int \mathcal{F}[e^{i\varphi_S(\mathbf{r})}](\mathbf{k})\hat{S}^\dagger_{\mathbf{K}+\mathbf{k}}d\mathbf{k}$, where $\mathcal{F}$ represents the Fourier transform in the spatial domain. With periodic $\varphi_S(\mathbf{r})$, the transformation becomes a Fourier series, realizing a multioutput SW beam splitter in two momentum-space dimensions.

We first select φ_S to be a sine wave $\varphi_S(y) = \chi\sin(k_g y + \vartheta)$, where k_g is the grating wave vector. For technical reasons, the sine modulation is accompanied by a constant component φ_0. With such modulation, all SWs are diffracted into subsequent orders with central y wave vector components $K_y + mk_g, m \in \mathbb{Z}$ and amplitudes of subsequent orders depending on strength of phase modulation quantified by its root-mean-square (rms) amplitude $\sqrt{\langle\varphi_S^2\rangle}$. For benchmarking, we generate a coherent SW state with excitation number $\bar{n} \approx 10^5$, by seeding the Raman process with a coherent state of light tuned to $|g\rangle \leftrightarrow |h\rangle$ two-photon transition along with the W laser. In Fig. 2(a), we depict wave-vector-resolved intensity of light emitted from the SWs as a function of phase modulation strength. By integrating the intensities in the discernible diffraction orders, we compare the experimental result with the expected behavior [Fig. 2(b)], finding excellent agreement and confirming the proposed mechanism for SW diffraction.

For the purpose of quantum engineering of SWs, we now show that through precise control of the phase modulation pattern we achieve desired amplitudes of diffraction orders, creating a controllable 1-to-N quantum network, where the zeroth order remains one of the output ports. Figures 2(c) and 2(d) depict the wave-vector-resolved SW density. With this we show that SWs are predominantly diffracted in the selected direction through a proper asymmetrical modulation, here composed of a sine wave with two frequencies with controlled relative phase.

With the SW modulation operating with high populations, we now evaluate its performance at the single excitation level. We probabilistically generate SWs heralded by detection of w photons on an I-sCMOS camera situated in the far field of the atomic ensemble. Quantum character of excitations is certified by the second-order

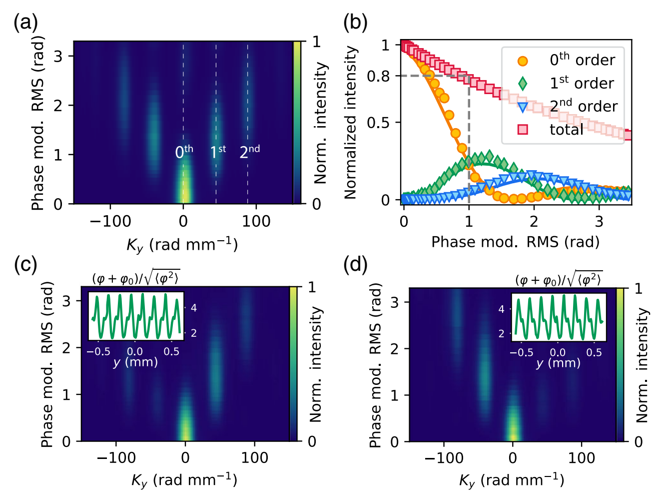

FIG. 2. Performance of the SW phase modulator. (a) Light intensity emitted from a SW as a function of a pure sine modulation rms amplitude $\sqrt{\langle\varphi_S^2\rangle}$ and the wave vector K_y component; (b) intensities in diffraction orders 0–2, marked in (a) along with the expected behavior (lines). In (c),(d) we change the modulation to include a term with higher frequency (insets: phase modulation patterns). Depending on the relative phase between the two terms, we observe diffraction predominantly in the selected direction.

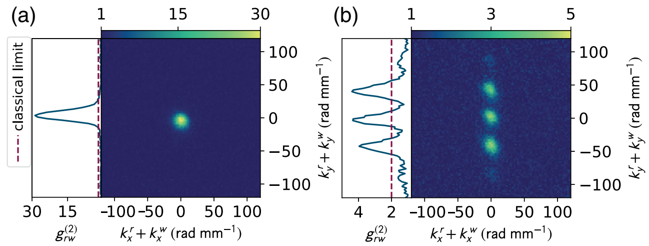

FIG. 3. A reference measurement (a) of second-order cross-correlation $g^{(2)}_{rw}$ reveals a single peak at $k^r_y + k^w_y = 0$, demonstrating momentum anticorrelations. By reshaping the SWs with a sine modulation pattern with wave vector k_g, we modify the correlation function (b) to feature two additional peaks at $k^r_y + k^w_y = \pm k_g$.

correlation function $g^{(2)}_{rw} = \langle \hat{n}_r \hat{n}_w \rangle / \langle \hat{n}_r \rangle \langle \hat{n}_w \rangle > 2$, which we express in terms of wave-vector-sum variables, taking advantage of wave vector multiplexing [22]. If the SWs are converted to photons without manipulation, a single peak at $k^r_x + k^w_x = k^r_y + k^w_y = 0$ is observed, as in Fig. 3(a), since in general $\mathbf{k}^w + \mathbf{k}^r = \mathbf{k}^W + \mathbf{k}^R$ and we select $\mathbf{k}^W_\perp = -\mathbf{k}^R_\perp$. With sinusoidal phase modulation with rms $= 1.0$ rad and wave vector k_g applied along the y direction during storage, the peak is split into three equal diffraction orders [Fig. 3(b)] with very little contribution to higher orders; thus we may write that the $\hat{S}_\mathbf{K}$ operator is transformed into a sum of three operators: $\hat{\tilde{S}}_\mathbf{K} = (\hat{S}_\mathbf{K} + e^{i\vartheta} \hat{S}_{\mathbf{K}+k_g \hat{e}_y} - e^{-i\vartheta} \hat{S}_{\mathbf{K}-k_g \hat{e}_y})/\sqrt{3}$. We certify quantum photon-number correlations in each peak, demonstrating that our modulation scheme preserves statistical properties of a SW, by operating with high efficiency and without adding spurious noise.

We now use the presented manipulation to observe interference of SWs. Following Fig. 4, using single-mode photon counting avalanche photodiodes (see Supplemental Material [39]) we select a pair of Gaussian-shaped modes (mode field radius $\sigma = 10.3$ rad mm^{-1}) for the w photon (wa and wb) corresponding to SW modes (ra and rb) with $K^{ra/rb}_y = \pm \Delta K_y / 2 = \pm 45$ rad mm^{-1} and equal $K^{ra}_x = K^{rb}_x \approx 200$ rad mm^{-1} ($\Delta K_x = 0$). By heralding a pair of w photons, we generate a SW pair $\hat{S}^\dagger_{ra} \hat{S}^\dagger_{rb} |0\rangle = |11\rangle_{ra,rb}$. With a proper phase modulation, each SW gets equally distributed into three equidistant modes. We select the grating period $k_g = \Delta K_y = 90$ rad mm^{-1}, so that after manipulation we may write operators for resulting modes rc and rd as $\hat{S}^\dagger_{rc} = (\hat{S}^\dagger_{ra} + e^{-i\vartheta} \hat{S}^\dagger_{rb} - e^{i\vartheta} \hat{S}^\dagger_{va})/\sqrt{3}$ and $\hat{S}^\dagger_{rd} = (\hat{S}^\dagger_{rb} + e^{-i\vartheta} \hat{S}^\dagger_{vb} - e^{i\vartheta} \hat{S}^\dagger_{ra})/\sqrt{3}$. Let us now assume that the modes are well overlapped, that is, $\Delta K_x = 0$ and $\Delta K_y = k_g$ and modes va and vb with $K^{va/vb}_y = \pm \frac{3}{2} \Delta K_y$ reside in vacuum (no excitation is heralded in these modes and we neglect their thermal occupations). With the output state given by $\hat{\rho}_{rc,rd} = 1/9 |00\rangle_{rc,rd} \langle 00| + 2/9 |01\rangle_{rc,rd} \langle 01| + 2/9 |10\rangle_{rc,rd} \langle 10| + 4/9 |\psi\rangle\langle\psi|$ with $|\psi\rangle = (e^{i\vartheta}|20\rangle + e^{-i\vartheta}|02\rangle)/\sqrt{2}$, the interference is observable in the heralded

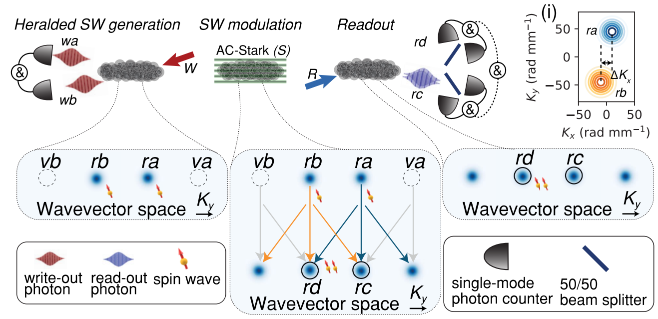

FIG. 4. The protocol for quantum interference of SWs. Detection of two w photons in modes wa and wb (selected through single-mode fibers) heralds generation of a SW pair in modes ra and rb. The three-way splitter is then used to interfere the two SWs. By detecting the SWs through photons converted to rc and rd modes, we observe bunching due to their bosonic nature. Inset (i) presents the input SW modes in the (K_x, K_y) plane. Photonic detection modes are always set to collect photons emitted from heralded SW modes.

cross-correlation $g^{(2)}_{rc,rd|wa,wb} = \langle \hat{n}_{rc} \hat{n}_{rd} \hat{n}_{wa} \hat{n}_{wb} \rangle \langle \hat{n}_{wa} \hat{n}_{wb} \rangle / \langle \hat{n}_{rc} \hat{n}_{wa} \hat{n}_{wb} \rangle \langle \hat{n}_{rd} \hat{n}_{wa} \hat{n}_{wb} \rangle$ counting coincidences between photons emitted from modes rc and rd—these coincidences vanish due to quantum interference. Simultaneously, the number of self-coincidences quantified by $g^{(2)}_{rc,rc|wa,wb}$ (or $g^{(2)}_{rd,rd|wa,wb}$) increases.

In the experiment, we first set $g^{(2)}_{wr} \approx 20$ and then apply the modulation that yields all cross-correlations, such as $g^{(2)}_{wa,rc} = g^{(2)}_{wa,rd} \approx 6$ [Fig. 5(c)]. The initial extrinsic readout efficiency, defined as the ratio of $w - r$ coincidences to the number of w counts is 4%, which corresponds to ~30% intrinsic memory efficiency after correcting for losses and detection efficiency. The efficiency of the modulation (at all discernible orders) is over 80%. With the initial coincidence $w - r$ rate of 40 Hz, we detect from 0.1 up to 0.5 quadruple coincidences per minute. With our current optical depth of 200 (as measured at the closed $F = 2 \rightarrow F = 3$ transition), we can achieve efficiencies of over 60% for classical pulses; however, since a large detuning and power of the R laser with ~1 μs long pulses is required, we currently achieve better overall performance at 30% efficiency with only 80 ns long pulses and the R laser tuned on resonance, which is mainly due to dark counts as well as filtration performance.

Figure 5(a) depicts the results obtained as we change the overlap between shifted modes by varying ΔK_x. If the modes are overlapping at $\Delta K_x = 0$, we obtain a value of $g^{(2)}_{rc,rd|wa,wb} = 0.20 \pm 0.06$, which certifies the observation of two-SW HOM interference. Simultaneously, taking the $g^{(2)}_{rc,rc|wa,wb}$ autocorrelation, we observe more than a two-fold increase from 0.5 ± 0.4 to 1.3 ± 0.2 compared with the case of nonoverlapping modes, showing that the pair of

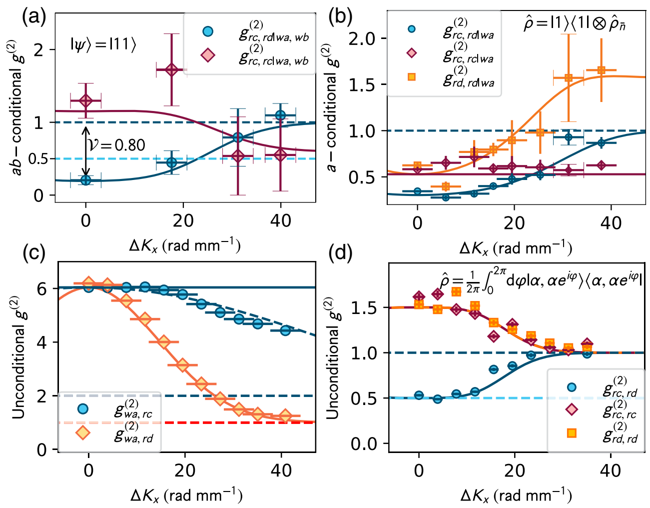

FIG. 5. Demonstration of quantum interference of SWs. (a) HOM dip as a function of mode wave vector separation. Bunching may be suppressed if the modes ra and rb are separated in the K_x direction of the momentum space. (b) By heralding only the w photon in the wa mode, we implement a HBT experiment, observing nonclassical statistics of the SW state. (c) The second-order correlation between w and r photons validating the operation of the three-way splitter with a slight drop in $g^{(2)}_{wa,rc}$ due to residual misalignment as the modes are moved (resulting in reduced fiber coupling efficiency). (d) HOM experiment for coherent input state with phase averaging. Vertical error bars correspond to one standard deviation inferred from Poissonian statistics of photon counts; horizontal error bars are due to mechanical precision of mode selection.

SWs is bunched and resides in a single mode. The theoretical prediction, detailed in the Supplemental Material [39], is made by first considering that each pair of contributing modes is squeezed to the same degree with the probability to generate a photon-SW pair $p = 0.05$, then implementing the given beam splitter network, and finally adding the influence of dark counts at the detection stage.

A distinct quantum protocol is implemented by postselecting only w photon detection events in the wa mode [Fig. 5(b)]. With this, we effectively implement a HBT measurement of a single SW in mode ra without optical beam splitting. The mode rb is modeled as containing a thermal state $\hat{\rho}_{rb}(\bar{n})$ with $\bar{n} = 0.1$. Value of $g^{(2)}_{rc,rd|wa} = 0.34 \pm 0.01 < 1$ clearly confirms the single excitation character. As the modes are decoupled, we observe a single photon statistic with $g^{(2)}_{rc,rc|wa} = 0.67 \pm 0.08 < 1$ for the rc mode and close to a single-mode thermal statistic with $g^{(2)}_{rd,rd|wa} = 1.65 \pm 0.34$ for the rd mode.

Finally, we directly populate the SW modes ra and rb with coherent state with population $\bar{n} = 0.1$. The classical analog of the HOM effect is observed [Fig. 5(d)] as we vary the phase offset of the ACS grating ϑ during a measurement, effectively creating a mixed state at the output. This corresponds to an interference of two phase-averaged coherent states that yield an anticorrelated behavior $g^{(2)}_{rc,rd} \to 0.5$ [9]. In the experiment, we indeed observe $g^{(2)}_{rc,rd} = 0.53 \pm 0.02$ at $\Delta K_x = 0$, which confirms the high visibility (47% out of 50% maximal). Note that a narrower distribution is observed in this case as we use a distinct mode function with $\sigma = 6.8$ rad mm^{-1}.

This demonstration of HOM interference of SWs not only exposes their bosonic nature, but paves the way towards implementing complex quantum operations, including more SW modes, that are the primitives of the linear-optical quantum computation scheme [76]. The only hitherto successful attempt at HOM interference of SWs relied on two different magnetic sublevels coupled through Raman transitions [77]. Such approach could also be extended to the spatial domain, yet we believe that the ACS modulation provides more versatility in terms of implemented operations due to inherent access to all wave vectors. Our experiment could furthermore greatly benefit from the deterministic SW generation protocol based on Rydberg blockade [77] to improve our current heralded SW pair generation rate. Furthermore, an ultrahigh optical density or cavity-based design [42,78,79] could bring the retrieval efficiency close to 90%. The combination of the gradient echo memory [63,80] and the ACS modulation could enable using SWs in the three-dimensional space, with their K_z component coupled with the photonic temporal degree of freedom (pulses arriving at different times) and transverse components of wave vectors paired with photonic transverse coordinates.

With the proposed techniques, a multiplexed source of heralded l photon can be realized [22,81] using a single atomic ensemble. A camera detector can herald creation of SWs in l out of M modes with wave vectors $(\mathbf{K}_1, \ldots, \mathbf{K}_l)$. Through adjustable ACS modulation, we then realize a switch redirecting these l populated modes into specific l output modes, with the success probability given by the incomplete regularized Beta function $I_{p\eta_w}(l, M - l + 1)\eta_r^l$ with $\eta_{w,r}$ being the efficiencies for detection of r and w photons. With $M \gtrsim l(1 + 3/\sqrt{l})/p\eta_w$ the probability approaches η_r^l and can dramatically beat the nonmultiplexed scenario, even with source operating at much higher rates (see Supplemental Material [39] for specific rate estimates).

The same idea can be used to design a multiplexed quantum repeater following the proposals presented in [29–31,45]. At the entanglement generation stage, we combine the optical fields coming from two nodes at a beam splitter and detect them with a camera. Detection of a w photon with wave vector k_w projects the pair of ensembles (A and B) into an entangled state $1/\sqrt{2}(\hat{S}^\dagger_{A,\mathbf{K}} + \hat{S}^\dagger_{B,\mathbf{K}})|0\rangle_A|0\rangle_B$, yet the generation rate can be high since we can keep a low probability to generate the state per mode, but achieve high rate per *any* mode. In a similar manner as in the multiplexed photon generation protocol, many states can be generated at the same time. At the entanglement connection stage, the entangled states are paired to form entangled qubits and then ACS modulation matches the SW modes of two ensembles being connected so entanglement can be established between them via HOM interference of r photons. Finally, with the ACS modulation we mix various entangled qubits stored in one ensemble to obtain purified pairs. This protocol corrects both for phase errors thanks to HOM interference and reduces errors in the logical space thanks to the entanglement purification step; yet, most importantly, it is inherently multiplexed and uses only a pair of atomic ensembles in each node (see Supplemental Material [39] for more details). More advanced error correction codes for quantum repeaters have already been proposed [19,32,82–84], but require a multiqubit quantum computer at each node. Such advanced quantum information processing capability is hard to achieve in practice with linear optics [76], but photons stored as Rydberg SWs for which nonlinear interactions can be engineered [52,85,86] could provide such capability when combined with our linear-operations scheme.

Current parameters of the demonstrated device already allow realization of original schemes, but can be improved by better use of wave vector multiplexing facilitating faster and nearly deterministic generation of single SWs and prompt transit towards realization of the proposed protocols. In conclusion, our fundamentally new scheme of SW manipulation along with potential derivative protocols lends itself to many applications in light technologies and potentially allows exploration of nonlinear interactions in the spatial domain.

We thank K. Banaszek for generous support and K. T. Kaczmarek, M. Jachura, and P. L. Knight for helpful discussions. This work has been funded by the National Science Centre, Poland (NCN) Grants No. 2015/19/N/ST2/01671, No. 2016/21/B/ST2/02559, No. 2017/25/N/ST2/01163, and No. 2017/25/N/ST2/00713 and by the Polish Ministry of Science and Higher Education (MNiSW) “Diamentowy Grant” projects No. DI2013 011943 and No. DI2016 014846. M. D. was supported by the Foundation for Polish Science. The research is supported by the Foundation for Polish Science, cofinanced by the European Union under the European Regional Development Fund, as a part of the “Quantum Optical Technologies” project carried out within the International Research Agendas programme.

M. P. and M. M. contributed equally to this work.

[*]michal.parniak@fuw.edu.pl
[†]mateusz.mazelanik@fuw.edu.pl

[1] C. K. Hong, Z. Y. Ou, and L. Mandel, Phys. Rev. Lett. **59**, 2044 (1987).
[2] A. M. Kaufman, B. J. Lester, C. M. Reynolds, M. L. Wall, M. Foss-Feig, K. R. A. Hazzard, A. M. Rey, and C. A. Regal, Science **345**, 306 (2014).
[3] R. Lopes, A. Imanaliev, A. Aspect, M. Cheneau, D. Boiron, and C. I. Westbrook, Nature (London) **520**, 66 (2015).
[4] B. B. Brandt, C. Yannouleas, and U. Landman, Phys. Rev. A **97**, 053601 (2018).
[5] K. Toyoda, R. Hiji, A. Noguchi, and S. Urabe, Nature (London) **527**, 74 (2015).
[6] S. Hong, R. Riedinger, I. Marinković, A. Wallucks, S. G. Hofer, R. A. Norte, M. Aspelmeyer, and S. Gröblacher, Science **358**, 203 (2017).
[7] R. W. Heeres, L. P. Kouwenhoven, and V. Zwiller, Nat. Nanotechnol. **8**, 719 (2013).
[8] J. S. Fakonas, H. Lee, Y. A. Kelaita, and H. A. Atwater, Nat. Photonics **8**, 317 (2014).
[9] J. Jin, J. A. Slater, E. Saglamyurek, N. Sinclair, M. George, R. Ricken, D. Oblak, W. Sohler, and W. Tittel, Nat. Commun. **4**, 2386 (2013).
[10] P. Chen, C. Shu, X. Guo, M. M. T. Loy, and S. Du, Phys. Rev. Lett. **114**, 010401 (2015).
[11] P. Qian, Z. Gu, R. Cao, R. Wen, Z. Y. Ou, J. F. Chen, and W. Zhang, Phys. Rev. Lett. **117**, 013602 (2016).
[12] Y. Y. Gao, B. J. Lester, Y. Zhang, C. Wang, S. Rosenblum, L. Frunzio, L. Jiang, S. M. Girvin, and R. J. Schoelkopf, Phys. Rev. X **8**, 021073 (2018).
[13] H. Vural, S. L. Portalupi, J. Maisch, S. Kern, J. H. Weber, M. Jetter, J. Wrachtrup, R. Löw, I. Gerhardt, and P. Michler, Optica **5**, 367 (2018).
[14] M. Zopf, T. Macha, R. Keil, E. Uruñuela, Y. Chen, W. Alt, L. Ratschbacher, F. Ding, D. Meschede, and O. G. Schmidt, Phys. Rev. B **98**, 161302 (2018).
[15] J. S. Lundeen, B. Sutherland, A. Patel, C. Stewart, and C. Bamber, Nature (London) **474**, 188 (2011).
[16] R. Chrapkiewicz, M. Jachura, K. Banaszek, and W. Wasilewski, Nat. Photonics **10**, 576 (2016).
[17] C. Reimer, M. Kues, P. Roztocki, B. Wetzel, F. Grazioso, B. E. Little, S. T. Chu, T. Johnston, Y. Bromberg, L. Caspani, D. J. Moss, and R. Morandotti, Science **351**, 1176 (2016).
[18] N. Maring, P. Farrera, K. Kutluer, M. Mazzera, G. Heinze, and H. de Riedmatten, Nature (London) **551**, 485 (2017).
[19] W. J. Munro, K. A. Harrison, A. M. Stephens, S. J. Devitt, and K. Nemoto, Nat. Photonics **4**, 792 (2010).
[20] D.-S. Ding, Z.-Y. Zhou, B.-S. Shi, and G.-C. Guo, Nat. Commun. **4**, 2527 (2013).
[21] Y.-F. Pu, N. Jiang, W. Chang, H.-X. Yang, C. Li, and L.-M. Duan, Nat. Commun. **8**, 15359 (2017).
[22] M. Parniak, M. Dąbrowski, M. Mazelanik, A. Leszczyński, M. Lipka, and W. Wasilewski, Nat. Commun. **8**, 2140 (2017).
[23] P. L. Kapitza and P. A. M. Dirac, Proc. Cambridge Philos. Soc. **29**, 297 (1933).
[24] R. Handbury Brown and R. Q. Twiss, Nature (London) **177**, 27 (1956).
[25] L. M. Duan, M. D. Lukin, J. I. Cirac, and P. Zoller, Nature (London) **414**, 413 (2001).
[26] R. Fickler, G. Campbell, B. Buchler, P. K. Lam, and A. Zeilinger, Proc. Natl. Acad. Sci. U.S.A. **113**, 13642 (2016).

[27] J. Wang, J.-Y. Yang, I. M. Fazal, N. Ahmed, Y. Yan, H. Huang, Y. Ren, Y. Yue, S. Dolinar, M. Tur, and A. E. Willner, Nat. Photonics **6**, 488 (2012).
[28] D. J. Richardson, J. M. Fini, and L. E. Nelson, Nat. Photonics **7**, 354 (2013).
[29] L. Jiang, J. M. Taylor, and M. D. Lukin, Phys. Rev. A **76**, 012301 (2007).
[30] Z.-B. Chen, B. Zhao, Y.-A. Chen, J. Schmiedmayer, and J.-W. Pan, Phys. Rev. A **76**, 022329 (2007).
[31] B. Zhao, Z.-B. Chen, Y.-A. Chen, J. Schmiedmayer, and J.-W. Pan, Phys. Rev. Lett. **98**, 240502 (2007).
[32] S. Muralidharan, J. Kim, N. Lütkenhaus, M. D. Lukin, and L. Jiang, Phys. Rev. Lett. **112**, 250501 (2014).
[33] J. G. Bartholomew, T. Zhong, J. M. Kindem, R. Lopez-Rios, J. Rochman, I. Craiciu, E. Miyazono, and A. Faraon, Phys. Rev. A **97**, 063854 (2018).
[34] T. Chanelière and G. Hétet, Opt. Lett. **40**, 1294 (2015).
[35] V. M. Acosta, K. Jensen, C. Santori, D. Budker, and R. G. Beausoleil, Phys. Rev. Lett. **110**, 213605 (2013).
[36] P. Staanum and M. Drewsen, Phys. Rev. A **66**, 040302 (2002).
[37] T. Moriyasu, D. Nomoto, Y. Koyama, Y. Fukuda, and T. Kohmoto, Phys. Rev. Lett. **103**, 213602 (2009).
[38] A. Leszczyński, M. Mazelanik, M. Lipka, M. Parniak, M. Dąbrowski, and W. Wasilewski, Opt. Lett. **43**, 1147 (2018).
[39] See Supplemental Material at http://link.aps.org/supplemental/10.1103/PhysRevLett.122.063604 for additional discussion of modulation efficiency and universality, details of enhanced photon generation and quantum repeater protocol, and details of the experimental setup and theoretical modeling, including Refs. [40–75].
[40] J. M. Lukens and P. Lougovski, Optica **4**, 8 (2017).
[41] H.-H. Lu, J. M. Lukens, N. A. Peters, O. D. Odele, D. E. Leaird, A. M. Weiner, and P. Lougovski, Phys. Rev. Lett. **120**, 030502 (2018).
[42] Y.-W. Cho, G. T. Campbell, J. L. Everett, J. Bernu, D. B. Higginbottom, M. T. Cao, J. Geng, N. P. Robins, P. K. Lam, and B. C. Buchler, Optica **3**, 100 (2016).
[43] G. Andersen, P. Gelsinger-Austin, R. Gaddipati, P. Gaddipati, and F. Ghebremichael, Opt. Express **22**, 9432 (2014).
[44] J. Ma, S. Masoodian, D. A. Starkey, and E. R. Fossum, Optica **4**, 1474 (2017).
[45] O. A. Collins, S. D. Jenkins, A. Kuzmich, and T. A. B. Kennedy, Phys. Rev. Lett. **98**, 060502 (2007).
[46] J.-W. Pan, S. Gasparoni, R. Ursin, G. Weihs, and A. Zeilinger, Nature (London) **423**, 417 (2003).
[47] S. Guha, Phys. Rev. Lett. **106**, 240502 (2011).
[48] A. Klimek, M. Jachura, W. Wasilewski, and K. Banaszek, J. Mod. Opt. **63**, 2074 (2016).
[49] K. Banaszek, Nat. Photonics **6**, 351 (2012).
[50] F. E. Becerra, J. Fan, G. Baumgartner, J. Goldhar, J. T. Kosloski, and A. Migdall, Nat. Photonics **7**, 147 (2013).
[51] Z. Hou, J.-F. Tang, J. Shang, H. Zhu, J. Li, Y. Yuan, K.-D. Wu, G.-Y. Xiang, C.-F. Li, and G.-C. Guo, Nat. Commun. **9**, 1414 (2018).
[52] D. Petrosyan, F. Motzoi, M. Saffman, and K. Mølmer, Phys. Rev. A **96**, 042306 (2017).
[53] M. J. Gullans, J. D. Thompson, Y. Wang, Q.-Y. Liang, V. Vuletić, M. D. Lukin, and A. V. Gorshkov, Phys. Rev. Lett. **117**, 113601 (2016).
[54] K. Jachymski, P. Bienias, and H. P. Büchler, Phys. Rev. Lett. **117**, 053601 (2016).
[55] M. F. Maghrebi, N. Y. Yao, M. Hafezi, T. Pohl, O. Firstenberg, and A. V. Gorshkov, Phys. Rev. A **91**, 033838 (2015).
[56] A. Kitaev, Ann. Phys. (Amsterdam) **303**, 2 (2003).
[57] M. Dąbrowski, M. Mazelanik, M. Parniak, A. Leszczyński, M. Lipka, and W. Wasilewski, Phys. Rev. A **98**, 042126 (2018).
[58] R. Chrapkiewicz, W. Wasilewski, and K. Banaszek, Opt. Lett. **39**, 5090 (2014).
[59] M. Lipka, M. Parniak, and W. Wasilewski, Appl. Phys. Lett. **112**, 211105 (2018).
[60] M. Dąbrowski, R. Chrapkiewicz, and W. Wasilewski, Opt. Express **22**, 26076 (2014).
[61] M. Lipka, M. Parniak, and W. Wasilewski, Appl. Phys. B **123**, 238 (2017).
[62] S. Zhang, J. F. Chen, C. Liu, S. Zhou, M. M. T. Loy, G. K. L. Wong, and S. Du, Rev. Sci. Instrum. **83**, 073102 (2012).
[63] M. Hosseini, B. M. Sparkes, G. Hétet, J. J. Longdell, P. K. Lam, and B. C. Buchler, Nature (London) **461**, 241 (2009).
[64] H. Bernien, S. Schwartz, A. Keesling, H. Levine, A. Omran, H. Pichler, S. Choi, A. S. Zibrov, M. Endres, M. Greiner, V. Vuletić, and M. D. Lukin, Nature (London) **551**, 579 (2017).
[65] B. M. Sparkes, M. Hosseini, G. Hétet, P. K. Lam, and B. C. Buchler, Phys. Rev. A **82**, 043847 (2010).
[66] A. Leszczyński, M. Parniak, and W. Wasilewski, Opt. Express **25**, 284 (2017).
[67] M. Auzinsh, D. Budker, and S. Rochester, *Optically Polarized Atoms: Understanding Light-Atom Interactions* (Oxford University, New York, 2010).
[68] M. Parniak and W. Wasilewski, Phys. Rev. A **91**, 023418 (2015).
[69] H. Paul, Rev. Mod. Phys. **54**, 1061 (1982).
[70] G. R. Hadley, Opt. Lett. **17**, 1743 (1992).
[71] M. Trippenbach, W. Wasilewski, P. Kruk, G. Bryant, G. Fibich, and Y. Band, Opt. Commun. **210**, 385 (2002).
[72] A. Couairon, E. Brambilla, T. Corti, D. Majus, O. de J. Ramírez-Góngora, and M. Kolesik, Eur. Phys. J. Spec. Top. **199**, 5 (2011).
[73] P. Farrera, G. Heinze, B. Albrecht, M. Ho, M. Chávez, C. Teo, N. Sangouard, and H. de Riedmatten, Nat. Commun. **7**, 13556 (2016).
[74] M. G. Raymer, J. Mod. Opt. **51**, 1739 (2004).
[75] J. Kołodyński, J. Chwedeńczuk, and W. Wasilewski, Phys. Rev. A **86**, 013818 (2012).
[76] T. D. Ladd, F. Jelezko, R. Laflamme, Y. Nakamura, C. Monroe, and J. L. O'Brien, Nature (London) **464**, 45 (2010).
[77] J. Li, M.-T. Zhou, B. Jing, X.-J. Wang, S.-J. Yang, X. Jiang, K. Mølmer, X.-H. Bao, and J.-W. Pan, Phys. Rev. Lett. **117**, 180501 (2016).
[78] X.-H. Bao, A. Reingruber, P. Dietrich, J. Rui, A. Dück, T. Strassel, L. Li, N.-L. Liu, B. Zhao, and J.-W. Pan, Nat. Phys. **8**, 517 (2012).
[79] Y.-F. Hsiao, P.-J. Tsai, H.-S. Chen, S.-X. Lin, C.-C. Hung, C.-H. Lee, Y.-H. Chen, Y.-F. Chen, I. A. Yu, and Y.-C. Chen, Phys. Rev. Lett. **120**, 183602 (2018).
[80] G. Hétet and D. Guéry-Odelin, New J. Phys. **17**, 073003 (2015).

[81] J. Nunn, N. K. Langford, W. S. Kolthammer, T. F. M. Champion, M. R. Sprague, P. S. Michelberger, X. M. Jin, D. G. England, and I. A. Walmsley, Phys. Rev. Lett. **110**, 133601 (2013).

[82] L. Jiang, J. M. Taylor, K. Nemoto, W. J. Munro, R. Van Meter, and M. D. Lukin, Phys. Rev. A **79**, 032325 (2009).

[83] A. N. Glaudell, E. Waks, and J. M. Taylor, New J. Phys. **18**, 093008 (2016).

[84] S. Muralidharan, L. Li, J. Kim, N. Lütkenhaus, M. D. Lukin, and L. Jiang, Sci. Rep. **6**, 20463 (2016).

[85] T. Peyronel, O. Firstenberg, Q.-Y. Liang, S. Hofferberth, A. V. Gorshkov, T. Pohl, M. D. Lukin, and V. Vuletić, Nature (London) **488**, 57 (2012).

[86] E. Distante, A. Padrón-Brito, M. Cristiani, D. Paredes-Barato, and H. de Riedmatten, Phys. Rev. Lett. **117**, 113001 (2016).